Correlated-hopping-induced topological order in an atomic mixture

Letter

Correlated-hopping-induced topological order in an atomic mixture

Ashirbad Padhan [1,2,3,*] Luca Barbiero,[4,†] and Tapan Mishra [1,2,‡]

[1]*School of Physical Sciences, National Institute of Science Education and Research, Jatni, Odisha 752050, India*
[2]*Homi Bhabha National Institute, Training School Complex, Anushaktinagar, Mumbai, Maharashtra 400094, India*
[3]*Laboratoire de Physique Théorique, Université de Toulouse, CNRS, UPS, France*
[4]*Institute for Condensed Matter Physics and Complex Systems, DISAT, Politecnico di Torino, 10129 Torino, Italy*

(Received 18 March 2025; accepted 23 June 2025; published 25 July 2025)

The large majority of topological phases in one-dimensional many-body systems are known to be inherited from the corresponding single-particle Hamiltonian. In this work, we go beyond this assumption and find a new example of topological order induced through specific interaction couplings. Specifically, we consider a fermionic mixture where one component experiences a staggered on-site potential and it is coupled through density-dependent hopping interactions to the other fermionic component. Crucially, by varying the sign of the staggered potential, we show that this latter fermionic component can acquire topological properties. Due to matrix product state simulations, we prove this result both at equilibrium by extracting the behavior of correlation functions and in an out-of-equilibrium scheme by employing a Thouless charge pumping. Notably, we further discuss how our results can be probed in quantum simulators made up of ultracold atoms. Our results reveal an important and alternative mechanism that can give rise to topological order.

DOI: 10.1103/lw8k-7h6p

Introduction. The search for systems exhibiting topological phases and phase transitions has led to several discoveries following the observation of the seminal quantum Hall effect in condensed matter [1–6]. Significant progress has been made in recent decades to obtain signatures of the topological phases and to understand the origin and stability of such phases in various systems [7–11]. Hallmarked by the gapped bulk spectrum, quantized topological invariants, and associated gapless edge modes, the topological phases have attracted a great deal of attention due to their fundamental and technological importance. This has led to their observations in various systems ranging from condensed-matter systems, optical systems, and metamaterials to mechanical systems [12–20].

One of the simplest systems that exhibits topological properties is the one-dimensional tight-binding model of free fermions with dimerized hopping, known as the Su-Schrieffer-Heeger (SSH) model [21–23]. A suitable choice of hopping dimerization of the fermions stabilizes a topological phase, which undergoes a transition to a trivial phase by specifically shaping the hopping dimerization. While the topological order in the SSH model is a feature of the single-particle Hamiltonian, such a scenario also persists in the presence of interactions [24–49]. Indeed, the topological properties appearing in most of the many-body systems are known to be inherited from single-particle models and in some cases depend on the specific choice of the interparticle interactions that indirectly favor the SSH-type phenomena [50–55]. In other words, the particles experience an induced hopping dimerization under proper conditions, leading to the topological phase. Now the question is whether such a topological phase and associated phase transition in a many-body system can be established without requiring its inheritance from the single-particle limit or through direct interparticle interactions.

In this Letter, we tackle this interesting question. Specifically, we propose a system of spinful fermions in a one-dimensional optical lattice with asymmetric density-dependent (DD) tunneling (i.e., the hopping of one component depends on the density of the other and not vice versa) in which a topological phase transition can be established. By subjecting one of the components to a staggered on-site potential and allowing the hopping of other component to depend on the density of the former, we show that the latter component acquires topological properties. The onset of the topological phase is strongly dependent on the sign of the staggered potential, resulting in a transition from the topological phase to the trivial phase at a point where the staggered on-site potential vanishes. We stress that the topological phase that appears in the system considered here is a pure many-body effect and is not inherited from the single-particle Hamiltonian.

Model. The model of spinful fermions with asymmetric DD tunneling is given by

$$H = -t_\uparrow \sum_i (c^\dagger_{i\uparrow} c_{i+1\uparrow} + \text{H.c.}) + \Delta_\uparrow \sum_i (-1)^i n_{i\uparrow} - t_\downarrow \sum_i n_{i\uparrow} (c^\dagger_{i\downarrow} c_{i+1\downarrow} + \text{H.c.}), \quad (1)$$

where $c_{i\sigma}$ is the fermionic annihilation operator for the component $\sigma \in (\uparrow, \downarrow)$ and $n_{i\sigma}$ is the respective number operator at the ith lattice site. While $t_\uparrow$ and $\Delta_\uparrow$ denote the hopping

*Contact author: padhanashirbad@gmail.com
†Contact author: luca.barbiero@polito.it
‡Contact author: mishratapan@niser.ac.in

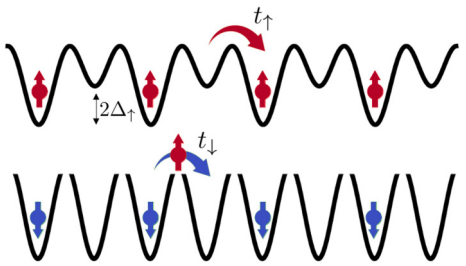

FIG. 1. Depiction of the model presented in Eq. (1) with hopping strengths $t_\uparrow$ and $t_\downarrow$ and on-site staggered potential strength $\Delta_\uparrow$. Here the $\uparrow$ component exhibits a superlattice behavior due to the staggered potential and the hopping of the $\downarrow$ component depends on the on-site density of the $\uparrow$ component.

and staggered on-site potential strengths of the $\uparrow$ component, respectively, $t_\downarrow$ fixes the hopping strength of the $\downarrow$ component. Note that here the hopping of the $\downarrow$ component depends on the site occupation of the $\uparrow$ component ($n_{i\uparrow}$), as shown in Fig. 1. The model considered above applies also to a system of two-component hard-core bosons.

For the model shown in Eq. (1), in the absence of the staggered on-site potential ($\Delta_\uparrow = 0$) and density dependence of the hopping of the $\downarrow$ component, the system consists of two decoupled gapless Luttinger liquids (LLs) of two individual components even at half filling. In this decoupled LL limit, any finite value of $\Delta_\uparrow$ will turn the $\uparrow$ component gapped, exhibiting a density-wave (DW)-type ordering ($\ldots 1\,0\,1\,0\ldots$) throughout the lattice. Surprisingly, at this point, if the hopping of the $\downarrow$ component is made to depend on the density of the $\uparrow$ component through the DD tunneling, then the $\downarrow$ component becomes gapped and turns topological if $\Delta_\uparrow > 0$. In the following, we discuss this phenomenon and associated topological phase transition in detail. Here we explore the ground-state properties of the model using the density-matrix renormalization-group method [56–58] based on the matrix product state ansatz [59,60] for a half-filled system, i.e., at density $\rho_\sigma = N_\sigma/L = 1/2$ on a system of L lattice sites, with N_σ the number of particles in each component. The algorithm is typically run for 15 sweeps with bond dimensions up to 500 per sweep. We perform all the numerical simulations by considering open boundary conditions and by fixing $t_\uparrow = t_\downarrow = 1$ as the energy unit.

Results. We first analyze the equilibrium properties of the system. As already mentioned, for any finite values of $\Delta_\uparrow$, the $\uparrow$ component is expected to form a gapped phase of DW-type ordering at half filling, i.e., at $\rho_\uparrow = 1/2$. Now, through the DD tunneling $t_\downarrow$, the properties of the $\downarrow$ component are strongly affected by the density of the $\uparrow$ particles. We confirm the gapped DW-type phase of the $\uparrow$ component by studying the system's gaps. To quantify them, we compute the single- and two-particle excitation gaps (or the charge gaps) of the system, which are defined as

$$G_{1\sigma} = E(N_\sigma + 1) + E(N_\sigma - 1) - 2E(N_\sigma) \tag{2}$$

and

$$G_{2\sigma} = E(N_\sigma + 2) + E(N_\sigma - 2) - 2E(N_\sigma), \tag{3}$$

respectively. Here $E(N_\sigma)$ is the ground-state energy, with N_σ the number of particles in each component. In Fig. 2(a) we

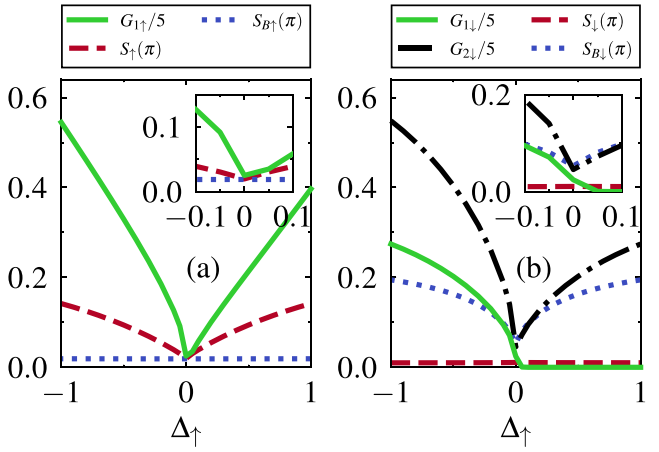

FIG. 2. (a) Single-particle charge gap $G_{1\uparrow}$ (green solid line), DW structure factor $S_\uparrow(\pi)$ (red dashed line), and BO structure factor $S_{B\uparrow}(\pi)$ (blue dotted line) plotted as a function of $\Delta_\uparrow$. (b) Single-particle charge gap $G_{1\downarrow}$ (green solid line), two-particle charge gap $G_{2\downarrow}$ (black dash-dotted line), DW structure factor $S_\downarrow(\pi)$ (red dashed line), and BO structure factor $S_{B\downarrow}(\pi)$ (blue dotted line) plotted as a function of $\Delta_\uparrow$. The insets show a zoomed-in view of the respective figures. Here we extrapolate the values of $G_{1,2\sigma}$ with system sizes $L = 40$, 60, 80, and 100 and consider $L = 100$ for the calculation of $S_\sigma(\pi)$ and $S_{B\sigma}(\pi)$. The charge gaps are scaled by a factor of 5 for better clarity. To avoid edge effects, the structure factors are calculated in the bulk of the lattice, i.e., in the range from $L/4$ to $3L/4$.

plot $G_{1\uparrow}$ as a function of $\Delta_\uparrow$ (green solid line). It can be seen that for all values of $\Delta_\uparrow$, the system becomes gapped even in the limit of $\Delta_\uparrow$ becoming zero [see the inset of Fig. 2(a)]. Due to the staggered on-site potential, the particles are expected to arrange themselves in a DW pattern due to doubling up of the unit cell. This behavior can be understood from the structure factor defined as

$$S_\sigma(k) = \frac{1}{L^2}\sum_{i,j} e^{ik|i-j|}\langle n_{i\sigma} n_{j\sigma}\rangle. \tag{4}$$

We plot $S_\uparrow(\pi)$ as a function $\Delta_\uparrow$ (red dashed line) in Fig. 2(a); it becomes finite as soon as the system becomes a gapped DW for any finite values of $\Delta_\uparrow$. Note that the finite structure factor is not a result of spontaneous symmetry breaking in the system but rather is due to the staggered on-site potential $\Delta_\uparrow$. Now we will show that this DW ordering in the $\uparrow$ component is the key to inducing topological features in the initially nontopological $\downarrow$ component through the DD tunneling.

For this purpose, we first monitor the behavior of the gap $G_{1\downarrow}$ as a function of $\Delta_\uparrow$, which is shown in Fig. 2(b). Contrary to the $\uparrow$ component case, it can be seen that $G_{1\downarrow}$ (green solid line) remains finite in the regime $\Delta_\uparrow \leqslant 0$ and vanishes when $\Delta_\uparrow > 0$. Such vanishing of the single-particle gap in the regime $\Delta_\uparrow > 0$ does not mean that the system is gapless but rather it is an indication of the existing edge modes within the gap at half filling. In such a situation, the gap in the system can be monitored by the two-particle gap $G_{2\downarrow}$ (black dash-dotted line), as shown in Fig. 2(b), which remains finite even for $\Delta_\uparrow > 0$. This behavior of the gap indicates a gapped-gapped transition as a function of $\Delta_\uparrow$ through $\Delta_\uparrow = 0$.

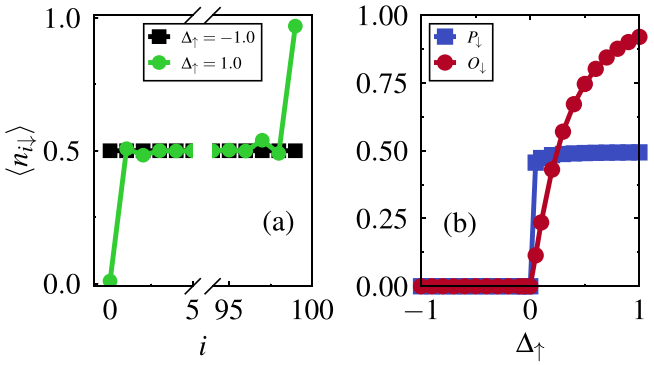

FIG. 3. (a) On-site densities $\langle n_{i\downarrow}\rangle$ plotted as a function of site index i for $\Delta_\uparrow = -1.0$ (black line with squares) and $\Delta_\uparrow = 1.0$ (green line with circles). (b) Polarization $P_\downarrow$ (blue line with squares) and string order parameter $O_\downarrow$ (red line with circles) plotted as a function of $\Delta_\uparrow$. Here the system size considered is $L = 100$.

We find that while the gaps in the $\uparrow$ component correspond to a DW-type ordering in the system, for the $\downarrow$ component they represent the dimerized or the bond-order (BO) phases. We prove the BO nature of the phase from the BO structure factor

$$S_{B\sigma}(k) = \frac{1}{L^2}\sum_{i,j} e^{\iota k|i-j|}\langle B_{i\sigma}B_{j\sigma}\rangle, \tag{5}$$

where $B_{i\sigma} = c^\dagger_{i\sigma}c_{i+1\sigma} + \text{H.c.}$ is the bond energy associated with the ith bond of the component σ. In Fig. 2(b) we plot $S_{B\downarrow}(\pi)$ (blue dotted line) as a function of $\Delta_\downarrow$, which exhibits finite values for $|\Delta_\uparrow| \neq 0$, indicating the BO nature of the gapped phases. To rule out the DW-type ordering as exhibited by the $\uparrow$ particles, we also plot $S_\downarrow(\pi)$ (red dashed line), which vanishes for all the values of $\Delta_\uparrow$. This confirms that the gapped phases for $|\Delta_\uparrow| \neq 0$ are the BO phases. Note that such bond ordering is absent for the $\uparrow$ particles, which can be seen from the vanishing values of $S_{B\uparrow}(\pi)$ (blue dotted line) in Fig. 2(a).

The above analysis clearly shows that the $\downarrow$ component develops bond ordering due to the DW-type structure in the $\uparrow$ component through the DD tunneling. Now the question is how the two BO phases on either side of $\Delta_\uparrow = 0$ in Fig. 2(b) are related to each other. In the following, we will show that while the BO phase for $\Delta_\uparrow > 0$ exhibits topological character, for $\Delta_\uparrow < 0$ it is a trivial BO phase, making the BO phases topologically distinct from each other.

Topological properties. Here we characterize the topological phase from the appearance of the edge states. As depicted in Fig. 3(a), the presence of degenerate edge states appears rather clearly by extracting the on-site densities $\langle n_{i\downarrow}\rangle$ (green circles) for positive values of $\Delta_\uparrow$. On the other hand, for negative values of $\Delta_\uparrow$, the system does not develop any edge states, as can be seen from the values of $\langle n_{i\downarrow}\rangle \sim 0.5$ (black squares) in Fig. 3(a). To quantify such topological character, we compute the edge state polarization defined by the formula

$$P_\sigma = \frac{1}{L}\sum_i (i - i_0)\langle\psi|n_{i\sigma}|\psi\rangle, \tag{6}$$

where $|\psi\rangle$ is the ground-state wave function and $i_0 = (L-1)/2$ is the center-of-mass position of the lattice [27]. This quantity is directly accessible in experiments through measuring the center-of-mass shift of the particle densities [13,14,61,62]. In Fig. 3(b) we plot $P_\downarrow$ as a function of $\Delta_\uparrow$, which shows that the polarization clearly vanishes at the critical point $\Delta_\uparrow = 0$ as well as in the BO phase for $\Delta_\uparrow < 0$. However, for $\Delta_\uparrow > 0$, the polarization assumes a constant value of $P_\downarrow \sim 0.5$. The finite value of polarization is usually attained when one of the edge lattice sites is filled and the other is not. However, when the particle density is uniformly distributed along the lattice, it becomes zero. Thus, $P_\downarrow$ together with the on-site density $\langle n_{i\downarrow}\rangle$ indirectly checks the existence of nontrivial edge states in a system. This indicates that the BO phase in the regime of $\Delta_\uparrow > 0$ is topological in nature. The topological BO phase is further quantified by the nonlocal string order parameter defined by

$$O_\sigma = -\left\langle z_{i\sigma}\exp\left(\iota\frac{\pi}{2}\sum_{k=i+1}^{j-1} z_{k\sigma}\right)z_{j\sigma}\right\rangle, \tag{7}$$

where $z_{i\sigma} = 1 - 2n_{i\sigma}$ [29,46,48,63–69] and the term in angular brackets denotes the expectation value over the ground state. Here we avoid the edge lattice sites and consider the maximum possible distance by choosing $i = 1$ and $j = L - 2$. In our case $O_\downarrow$ (red circles) becomes finite in the topological BO phase (for $\Delta_\uparrow > 0$) but vanishes elsewhere, as shown in Fig. 3(b).

These findings reveal that while the DD tunneling turns the $\downarrow$ component into a BO phase, depending on the sign of $\Delta_\uparrow$, the BO phase can be either trivial ($\Delta_\uparrow < 0$) or topological ($\Delta_\uparrow > 0$) in nature and hence a trivial to topological phase transition occurs as a function of $\Delta_\uparrow$ through the critical point at $\Delta_\uparrow = 0$. Such a nontrivial transformation of a nontopological phase to a topological phase is due to the interplay of the on-site staggered potential and the DD tunneling, which can be understood from the following arguments.

Due to the difference in the chemical potentials (or on-site energies) on alternate lattice sites, the $\uparrow$ particles get trapped in the deeper lattice sites, i.e., the sites with negative potentials. On the other hand, the hopping along the ith bond of the $\downarrow$ component becomes finite only if the density at the ith lattice site of the $\uparrow$ component is finite. Thus, disconnected dimers of $\downarrow$ component are formed, resulting in a fully dimerized effective SSH model.[1] Therefore, depending on whether the first site is empty or filled for the $\uparrow$ component due to the choice of $\Delta_\uparrow$, the $\downarrow$ component becomes topological or trivial in nature. This picture can be clearly understood from the average nearest-neighbor inter- and intracell density-density correlation functions defined as

$$C_{1\sigma} = \frac{1}{L}\sum_{i\in\text{odd}}\langle n_{i\sigma}n_{i+1\sigma}\rangle \tag{8}$$

[1]In the limit $\Delta_\uparrow \gg t_\uparrow$, the effective dimerized SSH model for the $\downarrow$ component can read $H^\downarrow_{\text{eff}} = -\frac{t_\downarrow}{2}\sum_i[1 - (-1)^i\frac{\Delta_\uparrow}{|\Delta_\uparrow|}](c^\dagger_{i\downarrow}c_{i+1\downarrow} + \text{H.c.})$.

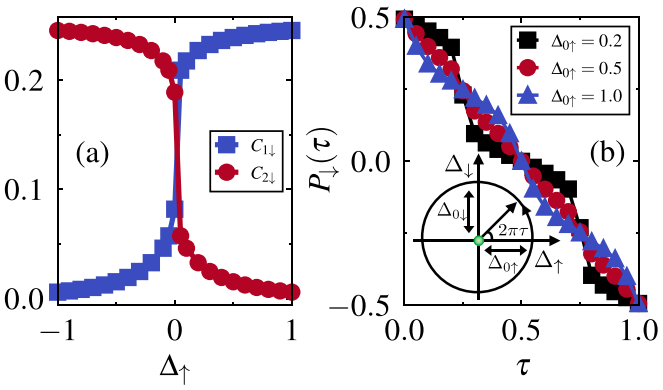

FIG. 4. (a) Inter- and intra-cell density-density correlations $C_{1\downarrow}$ (blue line with squares) and $C_{2\downarrow}$ (red line with circles) plotted as a function of $\Delta_\uparrow$. To avoid edge effects, $C_{1\downarrow}$ and $C_{2\downarrow}$ are calculated in the bulk of the lattice, i.e., in the range from $L/4$ to $3L/4$. (b) Polarization $P_\downarrow$ plotted as a function of the pumping parameter τ for $\Delta_{0\uparrow} = 0.2$ (black line with squares), 0.5 (red line with circles), and 1.0 (blue line with triangles). Here we fix $\Delta_{0\downarrow} = 0.5$ and consider a system of size $L = 100$. The inset shows the pumping scheme in the $\Delta_\uparrow$-$\Delta_\downarrow$ plane where the green dot marks the critical point, i.e., $(\Delta_\uparrow, \Delta_\downarrow) = (0, 0)$.

and

$$C_{2\sigma} = \frac{1}{L} \sum_{i \in \text{even}} \langle n_{i\sigma} n_{i+1\sigma} \rangle, \tag{9}$$

respectively. Since the intercell (intracell) correlation is dominant in the topological (trivial) BO phase, $C_{1\downarrow}$ ($C_{2\downarrow}$) is expected to become finite. From Fig. 4(a) we can notice that $C_{1\downarrow}$ (blue squares) remains very small for all the values of $\Delta_\uparrow < 0$. After the critical point, i.e., for $\Delta_\uparrow > 0$, there is a sharp increase in $C_{1\downarrow}$, indicating the topological BO phase. At the same time $C_{2\downarrow}$ (red circles) behaves just the opposite way to $C_{1\downarrow}$.

After discussing the equilibrium scenarios, in the remainder of the paper we explore the signatures of the topological phase transition through Thouless charge pumping.

Thouless pumping. Thouless charge pumping or the topological charge pumping (TCP) deals with the quantized transport of particles in a topological system through an adiabatic periodic modulation of system parameters. Moreover, they not only can probe the topological phase transitions but also provide a unique platform for a possible experimental probing [13,24,25,27,42,50,70–102]. In the following, we propose a pumping scheme to capture the topological phase transition of the $\downarrow$ component described in the preceding section. We define the pumping Hamiltonian in the spirit of the Rice-Mele model [103,104] as

$$H_p = -t_\uparrow \sum_i (c^\dagger_{i\uparrow} c_{i+1\uparrow} + \text{H.c.}) + \Delta_\uparrow \sum_i (-1)^i n_{i\uparrow} - t_\downarrow \sum_i n_{i\uparrow} (c^\dagger_{i\downarrow} c_{i+1\downarrow} + \text{H.c.}) + \Delta_\downarrow \sum_i (-1)^i n_{i\downarrow}, \tag{10}$$

where the first three terms are the same as Eq. (1) and the last term is an extra staggered on-site potential term associated with the $\downarrow$ component. The periodic modulation of the on-site potentials are achieved as $\Delta_\uparrow = \Delta_{0\uparrow} \cos(2\pi\tau)$ and $\Delta_\downarrow = \Delta_{0\downarrow} \sin(2\pi\tau)$. When the pumping parameter τ, which is equivalent to time, is varied from 0 to 1, a closed path in the parameter space is achieved, as shown in the inset of Fig. 4(b). To this end, we propose a pumping scheme involving these two on-site terms and consider three pumping cycles in the $\Delta_\uparrow$-$\Delta_\downarrow$ plane so that the path encloses the critical point $(\Delta_\uparrow, \Delta_\downarrow) = (0, 0)$. The three cycles have the parameters $\Delta_{0\uparrow} = 0.2$, 0.5, and 1.0, respectively, and $\Delta_{0\downarrow} = 0.5$ for all the cycles.

We characterize the TCP through the edge polarization using Eq. (6), where the ground state $|\psi(\tau)\rangle$ is computed as a function of τ. The polarization is related to the total amount of pumped charge per cycle as $Q_\sigma = \int_0^1 d\tau\, \partial_\tau P_\sigma(\tau)$, which takes quantized values if all the criteria for a robust pumping are satisfied. In Fig. 4(b) we plot $P_\downarrow(\tau)$ for $\Delta_{0\uparrow} = 0.2$, which shows a smooth variation from 0.5 to -0.5, thus a total pumped charge of $|Q_\downarrow| = 1$. Similarly, for both $\Delta_{0\uparrow} = 0.5$ and 1.0, the polarization varies smoothly, which signifies a quantized and robust charge pumping. This clearly indicates that the $\downarrow$ component exhibits a topological to trivial transition as $\Delta_\uparrow$ varies from negative to positive values through the critical point at $\Delta_\uparrow = 0$.

Conclusion. We have proposed a model of spinful fermions in one dimension where a topological phase can be stabilized through the correlated tunneling. By imposing a staggered on-site potential on one of the components, we have shown that a topological phase can be induced in the other component if the hopping of the latter component depends on the on-site density of the former component. Such an induced topological phase in turn results in a phase transition from a trivial BO phase to a topological BO phase as a function of the on-site staggered potential. While the topological and trivial phases exhibit characteristics similar to the ones exhibited by the SSH model, the phase transition does not occur through a gap closing point. Moreover, the bond ordering in this case arises from the competing effects of the on-site potential and the density-dependent tunneling as opposed to the dimerized hopping in the SSH model.

It is crucial to underline that, while on one hand, our results reveal a novel mechanism to generate topological phases, on the other, our results can be of crucial relevance also from an experimental perspective. It is indeed important to stress that, contrary to previous proposals [46], our scheme works for finite systems in the presence of boundaries. This represents an important aspect, as this is the usual configuration in quantum simulators made up of ultracold atoms in optical lattices which can allow both for the experimental realization of the model in Eq. (1) and for an efficient probing of its phase diagram. More specifically, resonant Floquet drivings of interacting atoms [105–108] combined with magnetic-field gradients or superlattice potentials have already paved the way towards the experimental realization of systems where the hopping of only one component is affected by the occupation of the other one [109–112]. In addition, staggered on-site potentials are largely implemented in ultracold-atom experiments [13,14,62,73], thus making it evident that the model in Eq. (1) might be promptly realized. Finally, through quantum gas microscopy [113], the on-site density can be measured with high accuracy. In such a way, the behavior of both the

edge state polarization (6) and the string correlator (7) can be probed in order to provide an accurate characterization of the topological properties of the system.

Acknowledgments. We thank Subhro Bhattacharjee for useful discussion. T.M. acknowledges support from Science and Engineering Research Board, Government of India, through Projects No. MTR/2022/000382 and No. STR/2022/000023. L.B. acknowledges financial support via the DiQut Grant No. 2022523NA7 funded by European Union Next Generation EU, PRIN 2022 program (Directorial Decree No. 104-02/02/2022 Ministero dell'Università e della Ricerca).

Data availability. The data that support the findings of this article are not publicly available upon publication because it is not technically feasible and/or the cost of preparing, depositing, and hosting the data would be prohibitive within the terms of this research project. The data are available from the authors upon reasonable request.

[1] K. v. Klitzing, G. Dorda, and M. Pepper, New method for high-accuracy determination of the fine-structure constant based on quantized Hall resistance, Phys. Rev. Lett. **45**, 494 (1980).

[2] D. J. Thouless, M. Kohmoto, M. P. Nightingale, and M. den Nijs, Quantized Hall conductance in a two-dimensional periodic potential, Phys. Rev. Lett. **49**, 405 (1982).

[3] M. Kohmoto, Topological invariant and the quantization of the Hall conductance, Ann. Phys. (NY) **160**, 343 (1985).

[4] R. B. Laughlin, Anomalous quantum Hall effect: An incompressible quantum fluid with fractionally charged excitations, Phys. Rev. Lett. **50**, 1395 (1983).

[5] F. D. M. Haldane, Model for a quantum Hall effect without Landau levels: Condensed-matter realization of the "parity anomaly", Phys. Rev. Lett. **61**, 2015 (1988).

[6] M. Z. Hasan and C. L. Kane, *Colloquium*: Topological insulators, Rev. Mod. Phys. **82**, 3045 (2010).

[7] C.-K. Chiu, J. C. Y. Teo, A. P. Schnyder, and S. Ryu, Classification of topological quantum matter with symmetries, Rev. Mod. Phys. **88**, 035005 (2016).

[8] X.-L. Qi and S.-C. Zhang, Topological insulators and superconductors, Rev. Mod. Phys. **83**, 1057 (2011).

[9] T. Senthil, Symmetry-protected topological phases of quantum matter, Annu. Rev. Condens. Matter Phys. **6**, 299 (2015).

[10] S. Rachel, Interacting topological insulators: A review, Rep. Prog. Phys. **81**, 116501 (2018).

[11] B. Wu, J. Song, J. Zhou, and H. Jiang, Disorder effects in topological states: Brief review of the recent developments, Chin. Phys. B **25**, 117311 (2016).

[12] M. Atala, M. Aidelsburger, J. T. Barreiro, D. Abanin, T. Kitagawa, E. Demler, and I. Bloch, Direct measurement of the Zak phase in topological Bloch bands, Nat. Phys. **9**, 795 (2013).

[13] S. Nakajima, T. Tomita, S. Taie, T. Ichinose, H. Ozawa, L. Wang, M. Troyer, and Y. Takahashi, Topological Thouless pumping of ultracold fermions, Nat. Phys. **12**, 296 (2016).

[14] M. Lohse, C. Schweizer, O. Zilberberg, M. Aidelsburger, and I. Bloch, A Thouless quantum pump with ultracold bosonic atoms in an optical superlattice, Nat. Phys. **12**, 350 (2016).

[15] S. Mukherjee, A. Spracklen, M. Valiente, E. Andersson, P. Öhberg, N. Goldman, and R. R. Thomson, Experimental observation of anomalous topological edge modes in a slowly driven photonic lattice, Nat. Commun. **8**, 13918 (2017).

[16] L. Lu, J. D. Joannopoulos, and M. Soljačić, Topological photonics, Nat. Photon. **8**, 821 (2014).

[17] L. Thatcher, P. Fairfield, L. Merlo-Ramírez, and J. M. Merlo, Experimental observation of topological phase transitions in a mechanical 1D-SSH model, Phys. Scr. **97**, 035702 (2022).

[18] E. J. Meier, F. A. An, and B. Gadway, Observation of the topological soliton state in the Su–Schrieffer–Heeger model, Nat. Commun. **7**, 13986 (2016).

[19] T. Kitagawa, M. A. Broome, A. Fedrizzi, M. S. Rudner, E. Berg, I. Kassal, A. Aspuru-Guzik, E. Demler, and A. G. White, Observation of topologically protected bound states in photonic quantum walks, Nat. Commun. **3**, 882 (2012).

[20] M. Leder, C. Grossert, L. Sitta, M. Genske, A. Rosch, and M. Weitz, Real-space imaging of a topologically protected edge state with ultracold atoms in an amplitude-chirped optical lattice, Nat. Commun. **7**, 13112 (2016).

[21] W. P. Su, J. R. Schrieffer, and A. J. Heeger, Solitons in polyacetylene, Phys. Rev. Lett. **42**, 1698 (1979).

[22] A. J. Heeger, S. Kivelson, J. R. Schrieffer, and W. P. Su, Solitons in conducting polymers, Rev. Mod. Phys. **60**, 781 (1988).

[23] J. K. Asbóth, L. Oroszlány, and A. Pályi, *A Short Course on Topological Insulators: Band Structure and Edge States in One and Two Dimensions*, Lecture Notes in Physics Vol. 919 (Springer, Cham, 2016), pp. 1–22.

[24] A. Hayward, C. Schweizer, M. Lohse, M. Aidelsburger, and F. Heidrich-Meisner, Topological charge pumping in the interacting bosonic Rice-Mele model, Phys. Rev. B **98**, 245148 (2018).

[25] M. Nakagawa, T. Yoshida, R. Peters, and N. Kawakami, Breakdown of topological Thouless pumping in the strongly interacting regime, Phys. Rev. B **98**, 115147 (2018).

[26] S. Mondal, S. Greschner, and T. Mishra, Three-body constrained bosons in a double-well optical lattice, Phys. Rev. A **100**, 013627 (2019).

[27] S. Greschner, S. Mondal, and T. Mishra, Topological charge pumping of bound bosonic pairs, Phys. Rev. A **101**, 053630 (2020).

[28] F. Grusdt, M. Höning, and M. Fleischhauer, Topological edge states in the one-dimensional superlattice Bose-Hubbard model, Phys. Rev. Lett. **110**, 260405 (2013).

[29] D. Wang, S. Xu, Y. Wang, and C. Wu, Detecting edge degeneracy in interacting topological insulators through entanglement entropy, Phys. Rev. B **91**, 115118 (2015).

[30] L. Barbiero, L. Santos, and N. Goldman, Quenched dynamics and spin-charge separation in an interacting topological lattice, Phys. Rev. B **97**, 201115(R) (2018).

[31] B. Sbierski and C. Karrasch, Topological invariants for the Haldane phase of interacting Su-Schrieffer-Heeger chains: Functional renormalization-group approach, Phys. Rev. B **98**, 165101 (2018).

[32] G. Magnifico, D. Vodola, E. Ercolessi, S. P. Kumar, M. Müller, and A. Bermudez, Symmetry-protected topological phases in

lattice gauge theories: Topological QED_2, Phys. Rev. D **99**, 014503 (2019).

[33] J. Sirker, M. Maiti, N. P. Konstantinidis, and N. Sedlmayr, Boundary fidelity and entanglement in the symmetry protected topological phase of the SSH model, J. Stat. Mech. (2014) P10032.

[34] T. Jin, P. Ruggiero, and T. Giamarchi, Bosonization of the interacting Su-Schrieffer-Heeger model, Phys. Rev. B **107**, L201111 (2023).

[35] A. M. Marques and R. G. Dias, Multihole edge states in Su-Schrieffer-Heeger chains with interactions, Phys. Rev. B **95**, 115443 (2017).

[36] X.-L. Yu, L. Jiang, Y.-M. Quan, T. Wu, Y. Chen, L.-J. Zou, and J. Wu, Topological phase transitions, Majorana modes, and quantum simulation of the Su–Schrieffer–Heeger model with nearest-neighbor interactions, Phys. Rev. B **101**, 045422 (2020).

[37] M. Yahyavi, L. Saleem, and B. Hetényi, Variational study of the interacting, spinless Su–Schrieffer–Heeger model, J. Phys.: Condens. Matter **30**, 445602 (2018).

[38] G. Salerno, M. Di Liberto, C. Menotti, and I. Carusotto, Topological two-body bound states in the interacting Haldane model, Phys. Rev. A **97**, 013637 (2018).

[39] M. Di Liberto, A. Recati, I. Carusotto, and C. Menotti, Two-body bound and edge states in the extended SSH Bose-Hubbard model, Eur. Phys. J.: Spec. Top. **226**, 2751 (2017).

[40] X. Zhou, J.-S. Pan, and S. Jia, Exploring interacting topological insulator in the extended Su-Schrieffer-Heeger model, Phys. Rev. B **107**, 054105 (2023).

[41] A. M. Marques and R. G. Dias, Topological bound states in interacting Su–Schrieffer–Heeger rings, J. Phys.: Condens. Matter **30**, 305601 (2018).

[42] S. Mondal, S. Greschner, L. Santos, and T. Mishra, Topological inheritance in two-component Hubbard models with single-component Su-Schrieffer-Heeger dimerization, Phys. Rev. A **104**, 013315 (2021).

[43] T. Yoshida, I. Danshita, R. Peters, and N. Kawakami, Reduction of topological $\mathbb{Z}$ classification in cold-atom systems, Phys. Rev. Lett. **121**, 025301 (2018).

[44] B.-T. Ye, L.-Z. Mu, and H. Fan, Entanglement spectrum of Su-Schrieffer-Heeger-Hubbard model, Phys. Rev. B **94**, 165167 (2016).

[45] Y. Kuno, Phase structure of the interacting Su-Schrieffer-Heeger model and the relationship with the Gross-Neveu model on lattice, Phys. Rev. B **99**, 064105 (2019).

[46] S. Julià-Farré, D. González-Cuadra, A. Patscheider, M. J. Mark, F. Ferlaino, M. Lewenstein, L. Barbiero, and A. Dauphin, Revealing the topological nature of the bond order wave in a strongly correlated quantum system, Phys. Rev. Res. **4**, L032005 (2022).

[47] N. H. Le, A. J. Fisher, N. J. Curson, and E. Ginossar, Topological phases of a dimerized Fermi–Hubbard model for semiconductor nano-lattices, npj Quantum Inf. **6**, 24 (2020).

[48] A. Montorsi, U. Bhattacharya, D. González-Cuadra, M. Lewenstein, G. Palumbo, and L. Barbiero, Interacting second-order topological insulators in one-dimensional fermions with correlated hopping, Phys. Rev. B **106**, L241115 (2022).

[49] B. Hetényi, Interaction-driven polarization shift in the t-v-V' lattice fermion model at half filling: Emergent Haldane phase, Phys. Rev. Res. **2**, 023277 (2020).

[50] S. Mondal, A. Padhan, and T. Mishra, Realizing a symmetry protected topological phase through dimerized interactions, Phys. Rev. B **106**, L201106 (2022).

[51] R. Parida, A. Padhan, and T. Mishra, Interaction driven topological phase transitions of hardcore bosons on a two-leg ladder, Phys. Rev. B **110**, 165110 (2024).

[52] H. Nigam, A. Padhan, D. Sen, T. Mishra, and S. Bhattacharjee, Phases and phase transitions in a dimerized spin-$\frac{1}{2}$ XXZ chain, Phys. Rev. B, **111**, 195131 (2025).

[53] R. Parida, D. Sen, and T. Mishra, Topological phase transition through tunable nearest-neighbor interactions in a one-dimensional lattice, arXiv:2502.14603.

[54] T. Chanda, R. Kraus, G. Morigi, and J. Zakrzewski, Self-organized topological insulator due to cavity-mediated correlated tunneling, Quantum **5**, 501 (2021).

[55] T. Chanda, R. Kraus, J. Zakrzewski, and G. Morigi, Bond order via cavity-mediated interactions, Phys. Rev. B **106**, 075137 (2022).

[56] S. R. White, Density matrix formulation for quantum renormalization groups, Phys. Rev. Lett. **69**, 2863 (1992).

[57] S. R. White, Density-matrix algorithms for quantum renormalization groups, Phys. Rev. B **48**, 10345 (1993).

[58] U. Schollwöck, The density-matrix renormalization group, Rev. Mod. Phys. **77**, 259 (2005).

[59] S. Rommer and S. Östlund, Class of ansatz wave functions for one-dimensional spin systems and their relation to the density matrix renormalization group, Phys. Rev. B **55**, 2164 (1997).

[60] U. Schollwöck, The density-matrix renormalization group in the age of matrix product states, Ann. Phys. (NY) **326**, 96 (2011).

[61] R. Citro and M. Aidelsburger, Thouless pumping and topology, Nat. Rev. Phys. **5**, 87 (2023).

[62] A.-S. Walter, Z. Zhu, M. Gächter, J. Minguzzi, S. Roschinski, K. Sandholzer, K. Viebahn, and T. Esslinger, Quantization and its breakdown in a Hubbard–Thouless pump, Nat. Phys. **19**, 1471 (2023).

[63] J. Fraxanet, D. González-Cuadra, T. Pfau, M. Lewenstein, T. Langen, and L. Barbiero, Topological quantum critical points in the extended Bose-Hubbard model, Phys. Rev. Lett. **128**, 043402 (2022).

[64] F. Anfuso and A. Rosch, String order and adiabatic continuity of Haldane chains and band insulators, Phys. Rev. B **75**, 144420 (2007).

[65] M. Endres, M. Cheneau, T. Fukuhara, C. Weitenberg, P. Schauss, C. Gross, L. Mazza, M. C. Bañuls, L. Pollet, I. Bloch, and S. Kuhr, Observation of correlated particle-hole pairs and string order in low-dimensional Mott insulators, Science **334**, 200 (2011).

[66] E. Haller, J. Hudson, A. Kelly, D. A. Cotta, B. Peaudecerf, G. D. Bruce, and S. Kuhr, Single-atom imaging of fermions in a quantum-gas microscope, Nat. Phys. **11**, 738 (2015).

[67] T. A. Hilker, G. Salomon, F. Grusdt, A. Omran, M. Boll, E. Demler, I. Bloch, and C. Gross, Revealing hidden antiferromagnetic correlations in doped Hubbard chains via string correlators, Science **357**, 484 (2017).

[68] S. de Léséleuc, V. Lienhard, P. Scholl, D. Barredo, S. Weber, N. Lang, H. P. Büchler, T. Lahaye, and A. Browaeys, Observation of a symmetry-protected topological phase of interacting bosons with Rydberg atoms, Science **365**, 775 (2019).

[69] A. Mazurenko, C. S. Chiu, G. Ji, M. F. Parsons, M. Kanász-Nagy, R. Schmidt, F. Grusdt, E. Demler, D. Greif, and M. Greiner, A cold-atom Fermi–Hubbard antiferromagnet, Nature (London) **545**, 462 (2017).

[70] H.-I. Lu, M. Schemmer, L. M. Aycock, D. Genkina, S. Sugawa, and I. B. Spielman, Geometrical pumping with a Bose-Einstein condensate, Phys. Rev. Lett. **116**, 200402 (2016).

[71] C. Schweizer, M. Lohse, R. Citro, and I. Bloch, Spin pumping and measurement of spin currents in optical superlattices, Phys. Rev. Lett. **117**, 170405 (2016).

[72] A. Fabre, J.-B. Bouhiron, T. Satoor, R. Lopes, and S. Nascimbene, Laughlin's topological charge pump in an atomic Hall cylinder, Phys. Rev. Lett. **128**, 173202 (2022).

[73] J. Minguzzi, Z. Zhu, K. Sandholzer, A.-S. Walter, K. Viebahn, and T. Esslinger, Topological pumping in a Floquet-Bloch band, Phys. Rev. Lett. **129**, 053201 (2022).

[74] L. Wang, M. Troyer, and X. Dai, Topological charge pumping in a one-dimensional optical lattice, Phys. Rev. Lett. **111**, 026802 (2013).

[75] Y. E. Kraus, Y. Lahini, Z. Ringel, M. Verbin, and O. Zilberberg, Topological states and adiabatic pumping in quasicrystals, Phys. Rev. Lett. **109**, 106402 (2012).

[76] M. Jürgensen, S. Mukherjee, and M. C. Rechtsman, Quantized nonlinear Thouless pumping, Nature (London) **596**, 63 (2021).

[77] M. Jürgensen, S. Mukherjee, C. Jörg, and M. C. Rechtsman, Quantized fractional Thouless pumping of solitons, Nat. Phys. **19**, 420 (2023).

[78] Q. Cheng, H. Wang, Y. Ke, T. Chen, Y. Yu, Y. S. Kivshar, C. Lee, and Y. Pan, Asymmetric topological pumping in non-paraxial photonics, Nat. Commun. **13**, 249 (2022).

[79] W. Liu, C. Wu, Y. Jia, S. Jia, G. Chen, and F. Chen, Observation of edge-to-edge topological transport in a photonic lattice, Phys. Rev. A **105**, L061502 (2022).

[80] Y. Ke, X. Qin, F. Mei, H. Zhong, Y. S. Kivshar, and C. Lee, Topological phase transitions and Thouless pumping of light in photonic waveguide arrays, Laser Photonics Rev. **10**, 995 (2016).

[81] W. Cheng, E. Prodan, and C. Prodan, Experimental demonstration of dynamic topological pumping across incommensurate bilayered acoustic metamaterials, Phys. Rev. Lett. **125**, 224301 (2020).

[82] I. H. Grinberg, M. Lin, C. Harris, W. A. Benalcazar, C. W. Peterson, T. L. Hughes, and G. Bahl, Robust temporal pumping in a magneto-mechanical topological insulator, Nat. Commun. **11**, 974 (2020).

[83] Z. Tao, W. Huang, J. Niu, L. Zhang, Y. Ke, X. Gu, L. Lin, J. Qiu, X. Sun, X. Yang *et al.*, Emulating Thouless pumping in the interacting Rice-Mele model using superconducting qutrits, Front. Phys. **20**, 33202 (2025).

[84] K. Viebahn, A.-S. Walter, E. Bertok, Z. Zhu, M. Gächter, A. A. Aligia, F. Heidrich-Meisner, and T. Esslinger, Interactions enable Thouless pumping in a nonsliding lattice, Phys. Rev. X **14**, 021049 (2024).

[85] Y. Hatsugai and T. Fukui, Bulk-edge correspondence in topological pumping, Phys. Rev. B **94**, 041102(R) (2016).

[86] R. Wang and Z. Song, Robustness of the pumping charge to dynamic disorder, Phys. Rev. B **100**, 184304 (2019).

[87] S. Hu, Y. Ke, and C. Lee, Topological quantum transport and spatial entanglement distribution via a disordered bulk channel, Phys. Rev. A **101**, 052323 (2020).

[88] Y. Kuno and Y. Hatsugai, Interaction-induced topological charge pump, Phys. Rev. Res. **2**, 042024(R) (2020).

[89] E. Bertok, F. Heidrich-Meisner, and A. A. Aligia, Splitting of topological charge pumping in an interacting two-component fermionic Rice-Mele Hubbard model, Phys. Rev. B **106**, 045141 (2022).

[90] S. Mondal, E. Bertok, and F. Heidrich-Meisner, Phonon-induced breakdown of Thouless pumping in the Rice-Mele-Holstein model, Phys. Rev. B **106**, 235118 (2022).

[91] Y.-T. Lin, D. M. Kennes, M. Pletyukhov, C. S. Weber, H. Schoeller, and V. Meden, Interacting Rice-Mele model: Bulk and boundaries, Phys. Rev. B **102**, 085122 (2020).

[92] J. Argüello-Luengo, M. J. Mark, F. Ferlaino, M. Lewenstein, L. Barbiero, and S. Julià-Farré, Stabilization of Hubbard-Thouless pumps through nonlocal fermionic repulsion, Quantum **8**, 1285 (2024).

[93] N. R. Cooper, J. Dalibard, and I. B. Spielman, Topological bands for ultracold atoms, Rev. Mod. Phys. **91**, 015005 (2019).

[94] T. Ozawa, H. M. Price, A. Amo, N. Goldman, M. Hafezi, L. Lu, M. C. Rechtsman, D. Schuster, J. Simon, O. Zilberberg, and I. Carusotto, Topological photonics, Rev. Mod. Phys. **91**, 015006 (2019).

[95] A. L. C. Hayward, E. Bertok, U. Schneider, and F. Heidrich-Meisner, Effect of disorder on topological charge pumping in the Rice-Mele model, Phys. Rev. A **103**, 043310 (2021).

[96] S. Nakajima, N. Takei, K. Sakuma, Y. Kuno, P. Marra, and Y. Takahashi, Competition and interplay between topology and quasi-periodic disorder in Thouless pumping of ultracold atoms, Nat. Phys. **17**, 844 (2021).

[97] Y.-P. Wu, L.-Z. Tang, G.-Q. Zhang, and D.-W. Zhang, Quantized topological Anderson-Thouless pump, Phys. Rev. A **106**, L051301 (2022).

[98] M. M. Wauters, A. Russomanno, R. Citro, G. E. Santoro, and L. Privitera, Localization, topology, and quantized transport in disordered Floquet systems, Phys. Rev. Lett. **123**, 266601 (2019).

[99] C. Lu, Z.-F. Cai, M. Zhang, H. Wang, Q. Ai, and T. Liu, Effects of disorder on Thouless pumping in higher-order topological insulators, Phys. Rev. B **107**, 165403 (2023).

[100] A. Cerjan, M. Wang, S. Huang, K. P. Chen, and M. C. Rechtsman, Thouless pumping in disordered photonic systems, Light Sci. Appl. **9**, 178 (2020).

[101] A. Padhan and T. Mishra, Quantized Thouless charge pumping in a system with onsite quasiperiodic disorder, Phys. Rev. B **109**, 174206 (2024).

[102] N. Mostaan, F. Grusdt, and N. Goldman, Quantized topological pumping of solitons in nonlinear photonics and ultracold atomic mixtures, Nat. Commun. **13**, 5997 (2022).

[103] M. J. Rice and E. J. Mele, Elementary excitations of a linearly conjugated diatomic polymer, Phys. Rev. Lett. **49**, 1455 (1982).

[104] J. K. Asbóth, L. Oroszlány, and A. Pályi, *A Short Course on Topological Insulators: Band Structure and Edge States in One and Two Dimensions* (Ref. [23]), pp. 55–68.

[105] A. R. Kolovsky, Creating artificial magnetic fields for cold atoms by photon-assisted tunneling, Europhys. Lett. **93**, 20003 (2011).

[106] Y.-A. Chen, S. Nascimbène, M. Aidelsburger, M. Atala, S. Trotzky, and I. Bloch, Controlling correlated tunneling and superexchange interactions with ac-driven optical lattices, Phys. Rev. Lett. **107**, 210405 (2011).

[107] N. Goldman, J. Dalibard, M. Aidelsburger, and N. R. Cooper, Periodically driven quantum matter: The case of resonant modulations, Phys. Rev. A **91**, 033632 (2015).

[108] M. Jamotte, N. Goldman, and M. Di Liberto, Strain and pseudo-magnetic fields in optical lattices from density-assisted tunneling, Commun. Phys. **5**, 30 (2022).

[109] A. Bermudez and D. Porras, Interaction-dependent photon-assisted tunneling in optical lattices: A quantum simulator of strongly-correlated electrons and dynamical gauge fields, New J. Phys. **17**, 103021 (2015).

[110] L. Barbiero, C. Schweizer, M. Aidelsburger, E. Demler, N. Goldman, and F. Grusdt, Coupling ultracold matter to dynamical gauge fields in optical lattices: From flux attachment to $\mathbb{Z}_2$ lattice gauge theories, Sci. Adv. **5**, eaav7444 (2019).

[111] C. Schweizer, F. Grusdt, M. Berngruber, L. Barbiero, E. Demler, N. Goldman, I. Bloch, and M. Aidelsburger, Floquet approach to $\mathbb{Z}_2$ lattice gauge theories with ultracold atoms in optical lattices, Nat. Phys. **15**, 1168 (2019).

[112] F. Görg, K. Sandholzer, J. Minguzzi, R. Desbuquois, M. Messer, and T. Esslinger, Realization of density-dependent Peierls phases to engineer quantized gauge fields coupled to ultracold matter, Nat. Phys. **15**, 1161 (2019).

[113] C. Gross and W. S. Bakr, Quantum gas microscopy for single atom and spin detection, Nat. Phys. **17**, 1316 (2021).